nature medicine

LETTERS

A high-throughput chemical screen reveals that harmine-mediated inhibition of DYRK1A increases human pancreatic beta cell replication

Peng Wang[1,2], Juan-Carlos Alvarez-Perez[1,2], Dan P Felsenfeld[3,4], Hongtao Liu[1], Sharmila Sivendran[3,4], Aaron Bender[1,2], Anil Kumar[1,2], Roberto Sanchez[3], Donald K Scott[1,2,5], Adolfo Garcia-Ocaña[1,2,5] & Andrew F Stewart[1,2]

Types 1 and 2 diabetes affect some 380 million people worldwide. Both ultimately result from a deficiency of functional pancreatic insulin-producing beta cells. Beta cells proliferate in humans during a brief temporal window beginning around the time of birth, with a peak percentage (~2%) engaged in the cell cycle in the first year of life[1–4]. In embryonic life and after early childhood, beta cell replication is barely detectable. Whereas beta cell expansion seems an obvious therapeutic approach to beta cell deficiency, adult human beta cells have proven recalcitrant to such efforts[1–8]. Hence, there remains an urgent need for antidiabetic therapeutic agents that can induce regeneration and expansion of adult human beta cells *in vivo* or *ex vivo*. Here, using a high-throughput small-molecule screen (HTS), we find that analogs of the small molecule harmine function as a new class of human beta cell mitogenic compounds. We also define dual-specificity tyrosine-regulated kinase-1a (DYRK1A) as the likely target of harmine and the nuclear factors of activated T cells (NFAT) family of transcription factors as likely mediators of human beta cell proliferation and differentiation. Using three different mouse and human islet *in vivo*–based models, we show that harmine is able to induce beta cell proliferation, increase islet mass and improve glycemic control. These observations suggest that harmine analogs may have unique therapeutic promise for human diabetes therapy. Enhancing the potency and beta cell specificity of these compounds are important future challenges.

The growth-mediating MYC proteins are key normal drivers of cell growth for many tissues[9–16] and lie downstream of numerous physiological, developmental and regenerative mitogenic signaling pathways[9–17]. More specifically, c-MYC is an essential driver of proliferation in Ins1 and RINm5F rat pancreatic beta cell lines and can drive human beta cell proliferation[17]. Reasoning that the *MYC* promoter might serve as a useful downstream 'sensor' for multiple diverse upstream signals leading to proliferation, we developed a luciferase-based small-molecule HTS strategy to detect molecules that directly or indirectly activate the *MYC* promoter in human cells (**Fig. 1a**, **Supplementary Fig. 1** and Online Methods).

We generated multiple stable cell lines expressing a luciferase reporter under control of the human *MYC* promoter. Among these, the human hepatocyte cell line HepG2 yielded the most robust luciferase responses and the least variability in pilot HTS screens, and we selected it for further screening using two small-molecule libraries: a library from the US Food and Drug Administration consisting of 2,300 small molecules and a 100,000-compound commercial library (see Online Methods). Of the 102,300 compounds tested, 4,500 scored >3 for median absolute deviation (MAD)[18] for luciferase activation (**Fig. 1b**). Among these, we assessed the 86 that generated the greatest normalized percentage activation (NPA >7.5%)[19] further for their ability both to induce c-MYC protein expression in HepG2 cells (**Supplementary Fig. 1**) and to induce BrdU incorporation in dispersed rat pancreatic beta cells (**Fig. 1c**). Only one compound, harmine, induced both a mild increase of c-MYC in HepG2 cells and substantial BrdU incorporation into rat beta cells. Harmine also induced BrdU incorporation and Ki-67 labeling in human beta cells, with the frequent appearance of double nuclei, suggesting recent cell division (**Fig. 1d–g**).

Harmine is a competitive inhibitor of ATP binding to the kinase pocket of DYRK1A, but it can also inhibit other DYRK family members, monoamine oxidases (MAOs) and cdc-like kinases (CLKs). We therefore surveyed additional harmine analogs[20–24] (**Fig. 2a**). Harmaline and harmane (inhibitors of MAO but not DYRK1A) did not induce proliferation; conversely, inhibitor of DYRK1A, (INDY, a chemical compound that inhibits DYRK1A but not MAO), activated proliferation in both rat and human beta cells (**Fig. 2b–d**), also yielding Ki-67$^+$ and BrdU$^+$ double nuclei (**Fig. 2d**). Harmine and INDY both also induced phosphorylation of histone H3, a third marker of cell cycle transition (**Supplementary Fig. 2**). Effective harmine and

[1]Diabetes, Obesity and Metabolism Institute, Icahn School of Medicine at Mount Sinai, New York, New York, USA. [2]Division of Endocrinology and Bone Disease, Icahn School of Medicine at Mount Sinai, New York, New York, USA. [3]Experimental Therapeutics Institute, Icahn School of Medicine at Mount Sinai, New York, New York, USA. [4]Integrated Screening Core, Icahn School of Medicine at Mount Sinai, New York, New York, USA. [5]Mindich Child Health and Development Institute, Icahn School of Medicine at Mount Sinai, New York, New York, USA. Correspondence should be addressed to A.F.S. (andrew.stewart@mssm.edu).

Received 30 June 2014; accepted 9 February 2015; published online 9 March 2015; doi:10.1038/nm.3820

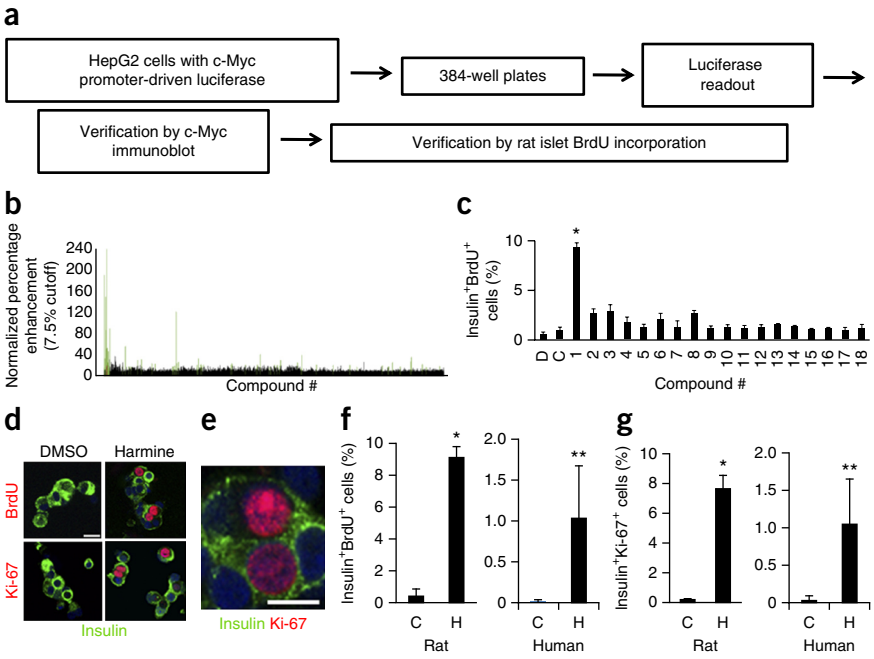

Figure 1 High-throughput screening reveals harmine family members as agonists of beta cell proliferation. (**a**) Schematic outline of the screen in HepG2 cells used to identify compounds that promote beta cell replication. See text and Online Methods for details. (**b**) Results of the primary screen showing the 4,500 initial hits (black) and the 86 compounds with a MAD score >3 (green). (**c**) Examples of tertiary screening (rat beta cell BrdU incorporation) of the 86 compounds. Compound 1 is harmine. "D" is DMSO, and "C" indicates rat islets treated with no vehicle. The BrdU screen was performed four times; where no error bars are seen, they are within the bar. (**d**) Representative examples (n = 10–20 images per donor; see Online Methods for a fuller explanation) of BrdU- and Ki-67–labeled human beta cells after treatment with harmine. Note BrdU and Ki-67 nuclear 'doublets' in human beta cells. See **f** and **g** descriptions for quantification regarding the total number of beta cells counted. (**e**) An enlarged view of harmine-treated human beta cells with Ki-67 nuclear doublets in adjacent cells. (**f**) Quantification of BrdU incorporation into rat (left) and human (right) beta cells. "C" indicates control (DMSO vehicle) and "H" harmine. A minimum of 1,000 beta cells was counted from multiple donors (n = 4 for rat, n = 6 for human) for each bar. (**g**) Quantification of Ki-67 labeling in rat and human beta cells. "C" indicates control (DMSO vehicle) and "H" harmine. A minimum of 1,000 beta cells was counted from multiple donor pairs (4 rat, 7 human) for each bar. In all relevant panels, error bars indicate sem *P < 0.05 and **P < 0.01, as determined by Wilcoxon rank test. Scale bars, 10 μm.

INDY doses were in the 1- to 15-μM range, with higher doses being detrimental to proliferation (**Fig. 2e–h**). WS6, a previously described small-molecule agonist of beta cell proliferation[25], had little effect on human beta cell proliferation in our hands (**Supplementary Fig. 3**). Ki-67 labeling induced by harmine was unaffected by glucose concentration (**Supplementary Fig. 2c**). Collectively, these observations suggested that DYRK1A or the closely related kinases DYRK1B, DYRK2 or CLKs 1 and 4, are the relevant targets of harmine and INDY. Harmine and INDY also activated proliferation in alpha and ductal cells, with no detectable proliferation in delta cells or pancreatic polypeptide cells (**Supplementary Fig. 3**).

We found no evidence of beta cell death or DNA damage in response to harmine or INDY as measured by TUNEL and p-γ-H2AX labeling (**Supplementary Fig. 2**). We did find that *INS* mRNA expression in harmine-treated human islets was higher than in vehicle-treated islets, but islet insulin content and glucose-stimulated insulin secretion were comparable between harmine- and INDY-treated islets and vehicle-treated controls (**Supplementary Fig. 4a–c**). Of note, we also found that the transcription factors PDX1, NKX6.1 and MAFA were increased at the mRNA and protein levels and showed potent staining in beta cells by immunocytochemistry (**Supplementary Fig. 4d–j**).

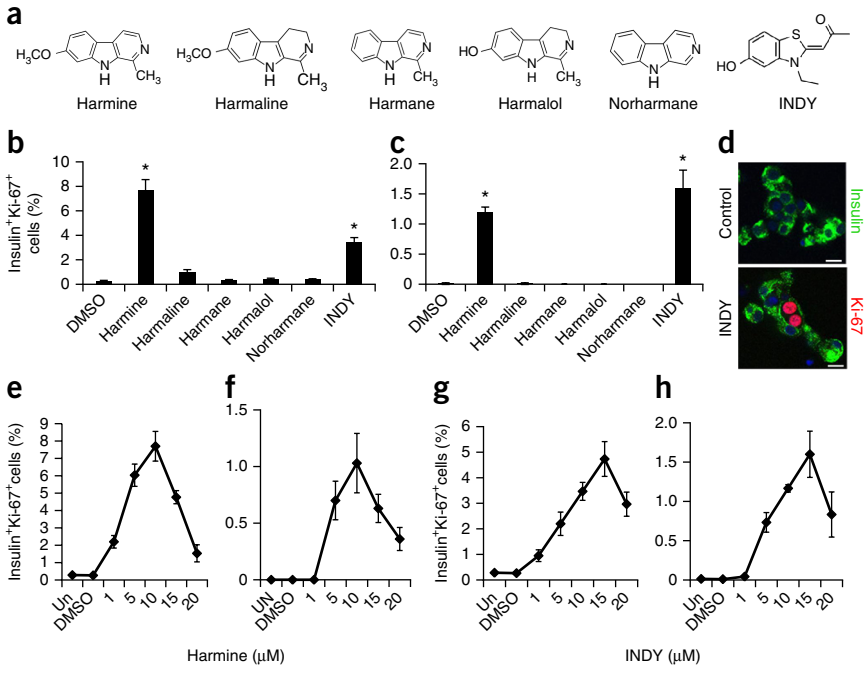

Figure 2 Structure-activity relationship analysis of harmine analogs on beta cell proliferation. (**a**) Chemical structures of structural or functional harmine analogs. (**b**,**c**) Quantification of Ki-67 labeling in rat (**b**, n = 4 donors) and human (**c**, n = 4 donors) beta cells in response to harmine analogs. (**d**) A representative example (n = 10–20 images per donor) from **b** of a Ki-67+ doublet induced by INDY. Scale bars, 10 μm. (**e**–**h**) Dose-response curves for harmine and INDY in rat (**e**,**g**) and human (**f**,**h**) beta cell Ki-67 labeling. In all relevant panels, error bars indicate sem *P < 0.05, as determined by Wilcoxon rank test. A minimum of 1,000 beta cells was counted from three rat or four human donors for each graph.

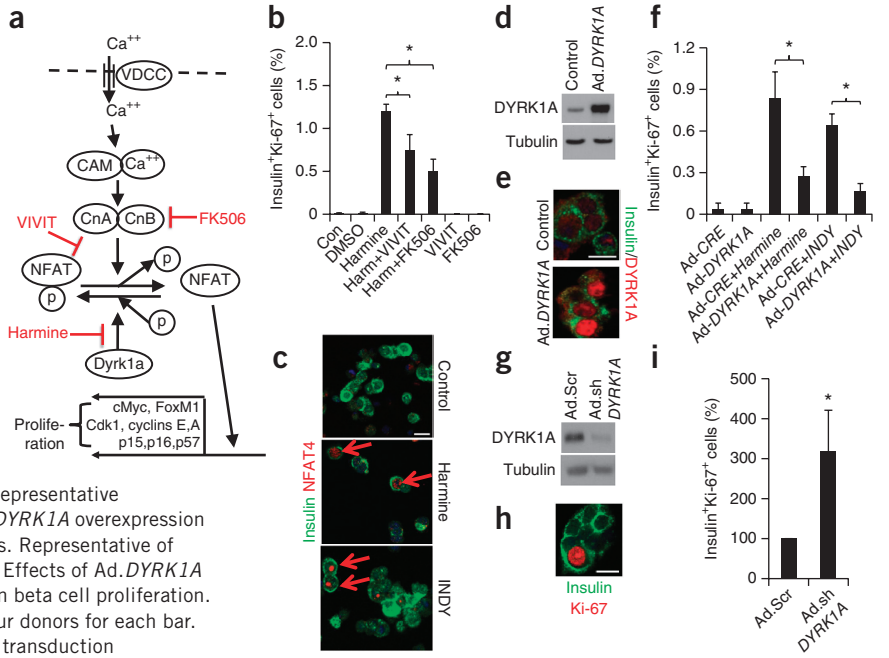

Figure 3 Calcineurin-NFAT-Dyrk1a signaling is implicated in harmine-induced beta cell proliferation. (**a**) A schematic diagram depicting the calcium (Ca^{2+})-calmodulin (CAM)-calcineurin (CnA and CnB subunits)-NFAT–c-MYC pathway regulating beta cell proliferation. The sites of action of harmine, VIVIT and FK506 are shown in red. (**b**) Beta cell proliferation in dispersed human islets in response to harmine, in the presence or absence of VIVIT or FK506 ($n = 4$ human preparations). (**c**) Representative images ($n = 10$–20 images per donor) of the effects of harmine (10 μM) or INDY (15 μM) treatment on NFAT4 translocation to the nucleus of human beta cells. Examples are shown by red arrows. Translocation of other NFATs is shown in **Supplementary Figure 7**. (**d**) Western blot of adenovirally mediated DYRK1A overexpression in human islets. Representative of experiments from three islet preparations. (**e**) Ad.*DYRK1A* overexpression and immunolabeling for DYRK1A in human beta cells. Representative of experiments from three human islet preparations. (**f**) Effects of Ad.*DYRK1A* overexpression on harmine- and INDY-induced human beta cell proliferation. A minimum of 1,000 beta cells was counted from four donors for each bar. (**g**) Western blot showing the effect of Ad.sh*DYRK1A* transduction compared to a scrambled shRNA control vector (Ad.Scr) on DYRK1A expression in human islets. Representative of four human islet preparations. (**h**) Representative image ($n = 10$–20 images per donor) of Ki-67 immunolabeling in human beta cells transduced with Ad.sh*DYRK1A*. (**i**) Quantification of Ki-67 in human beta cells transduced with Ad.sh*DYRK1A*. A minimum of 1,000 beta cells was counted from five donors for each bar. Scale bars, 10 μm. Error bars indicate sem $*P < 0.05$ as determined by Wilcoxon rank test.

To determine whether calcineurin-NFAT signaling[26–28] might mediate the proliferative effects of harmine analogs in rat and human beta cells (**Fig. 3a**), we blocked the NFAT-calcineurin interaction with the NFAT inhibitor VIVIT and inhibited calcineurin activity with FK-506. Both inhibitors attenuated Ki-67 labeling in both rat and human beta cells (**Fig. 3b** and **Supplementary Fig. 5**), suggesting a role for calcineurin-NFAT signaling in the effects of harmine and INDY on beta cell proliferation. We therefore surveyed the presence and subcellular localization of NFAT family members in human beta cells. As predicted by prior studies in rodent beta cells[27–29] and human beta cell RNA sequencing–based studies[30], NFATs were also detectable in the cytoplasm in quiescent human beta cells (**Supplementary Fig. 6**). Both harmine and INDY induced nuclear translocation of all four endogenous NFATs (**Fig. 3c** and **Supplementary Fig. 6**). Concordantly, adenovirally expressed NFAT2 (encoded by *NFATC1*) fused to GFP was readily apparent in the cytoplasm in vehicle-treated beta cells but shifted to a predominantly nuclear location within harmine- and INDY-treated beta cells (**Supplementary Fig. 7**).

To further explore whether DYRK1A is a relevant regulator of proliferation in human beta cells, we adenovirally overexpressed DYRK1A in human islets. Notably, though endogenous DYRK1A was detectable in normal quiescent human islets, DYRK1A could effectively be overexpressed, appearing in the nuclear compartment (**Fig. 3d**,**e**); its overexpression competitively attenuated harmine- and INDY-induced human beta cell proliferation (**Fig. 3f**). Conversely, reducing endogenous DYRK1A expression using an adenoviral shRNA directed against human *DYRK1A* led to a threefold higher degree of proliferation of the human beta cells as compared to a scrambled shRNA–expressing control adenovirus (**Fig. 3g–i**).

Harmine and INDY occupy the ATP-binding pocket of DYRK1A, forming two hydrogen bonds with the side chain of Lys188 and the backbone of Leu241, with hydrogen bond acceptor groups in the correct orientation to form these interactions[20–24] (**Supplementary Fig. 7**). Conversely, harmine analogs that lack DYRK1A inhibitory activity and beta cell mitogenic activity (**Fig. 2**) are expected to fail to bind within the ATP-binding pocket of DYRK1A because they lack one of the hydrogen bond acceptor groups (harmane, norharmane) or because the hydrogen bond acceptor groups are not correctly positioned (harmaline, harmalol) owing to their non-planar conformation.

As the HTS was based on *MYC* activation in HepG2 cells, we next asked whether harmine-induced proliferation of human islets required c-MYC activity. Harmine induced a reproducible but moderate (twofold) higher level of c-MYC protein in human islets as compared to vehicle-treated islets, and the c-MYC inhibitor 1RH (ref. 31) inhibited harmine-induced proliferation (**Supplementary Fig. 8a–d**). Further, adenoviral Cre–mediated excision of *Myc* from islets of $Myc^{loxP/loxP}$ mice[32] attenuated harmine-induced proliferation (**Supplementary Fig. 8e–h**). Thus, harmine-induced proliferation depends in part on c-MYC activation. Next, to find additional downstream cell cycle mediators of harmine analog action, we performed an mRNA screen of G1/S cell cycle control molecules, which we confirmed by immunoblot and immunocytochemistry. We found higher expression of relevant cyclins and cdks (e.g., cyclins A and E, CDK1, FOXM1, CDC25A, and E2Fs 1 and 2) and lower expression of cell cycle inhibitors (notably, $p15^{INK4}$, $p16^{INK4}$ and $p57^{CIP2}$) in islets treated with harmine or INDY as compared to vehicle-treated islets (**Supplementary Fig. 9**).

Finally, we used three different *in vivo* animal models to assess the ability of harmine to activate proliferation, augment beta cell mass and enhance glycemic control. In the first, a partial pancreatectomy (PPX) model, harmine treatment induced Ki-67 labeling in beta cells in both sham-operated mice and in mice subjected to PPX, with the most robust proliferation in the beta cells of harmine-treated PPX

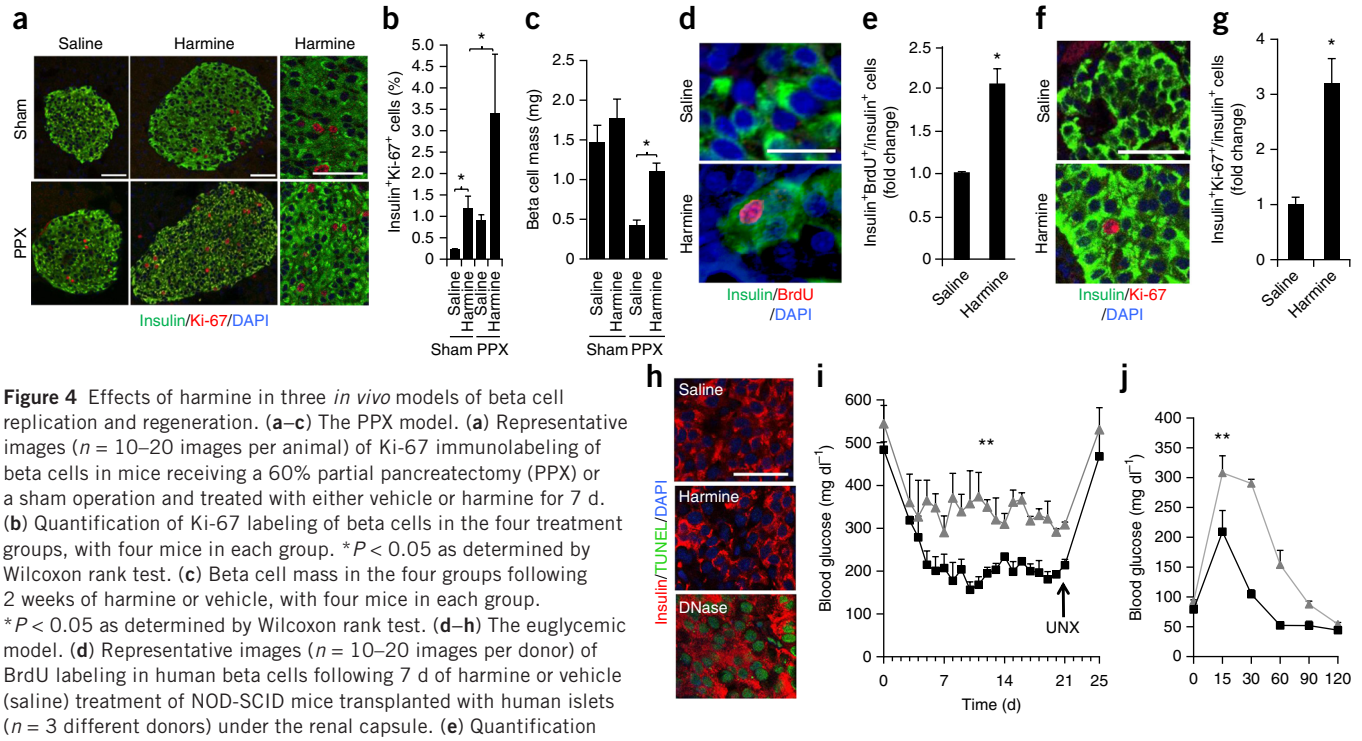

Figure 4 Effects of harmine in three *in vivo* models of beta cell replication and regeneration. (**a**–**c**) The PPX model. (**a**) Representative images (n = 10–20 images per animal) of Ki-67 immunolabeling of beta cells in mice receiving a 60% partial pancreatectomy (PPX) or a sham operation and treated with either vehicle or harmine for 7 d. (**b**) Quantification of Ki-67 labeling of beta cells in the four treatment groups, with four mice in each group. $^*P < 0.05$ as determined by Wilcoxon rank test. (**c**) Beta cell mass in the four groups following 2 weeks of harmine or vehicle, with four mice in each group. $^*P < 0.05$ as determined by Wilcoxon rank test. (**d**–**h**) The euglycemic model. (**d**) Representative images (n = 10–20 images per donor) of BrdU labeling in human beta cells following 7 d of harmine or vehicle (saline) treatment of NOD-SCID mice transplanted with human islets (n = 3 different donors) under the renal capsule. (**e**) Quantification of BrdU incorporation into transplanted human beta cells in the NOD-SCID mice in **d**. $^*P < 0.05$ as determined by Student's unpaired t-test. (**f**) Representative images (n = 10–20 images per donor) of Ki-67 immunolabeling of human beta cells in the same experiment as in **d**. (**g**) Quantification of Ki-67 immunolabeling in human beta cells in **d** (n = 3 different human islet grafts into NOD-SCID mice). $^*P < 0.05$ as determined by Student's unpaired t-test. (**h**) Representative images (n = 10–20 images per donor) of TUNEL labeling of the same three human islet grafts in **d**; DNase treatment is a positive control; no TUNEL$^+$ cells were observed in >1,000 insulin$^+$ cells counted. (**i**) The diabetic model: streptozotocin-diabetic NOD-SCID mice transplanted with human islets, treated for 14 d with saline (gray lines, n = 3 different mice transplanted with human islets from different donors) or harmine (black lines, n = 4 mice transplanted with human islets). Grafts were harvested at day 21 by unilateral nephrectomy (UNX). $^{**}P < 0.01$ for area under the curve as determined using unpaired Student's two-tailed t-test. (**j**) Intraperitoneal glucose tolerance test on day 20 in the same mice as in **i**. ** as in **i**. In all relevant panels, bars show mean ± sem Scale bars, 50 µm.

mice (**Fig. 4a**,**b**). In the PPX model, regeneration of beta cell mass was substantially more rapid in the harmine-treated mice than in the controls, reaching near-normal values in only 14 d (**Fig. 4c**). In the second model, a euglycemic nonobese diabetic–severe combined immunodeficiency (NOD-SCID) mouse model, BrdU and Ki-67 labeling was two- to threefold higher in human beta cells transplanted into the renal capsule of harmine-treated compared to control euglycemic mice, without evidence of beta cell death (**Fig. 4d**–**h**). In the third model, a marginal mass human islet transplant model in streptozotocin-diabetic NOD-SCID mice, harmine treatment also resulted in near normal glycemic control, as assessed both by postprandial and fasting glucose values and by intraperitoneal glucose tolerance challenge (**Fig. 4i**,**j**).

Harmine and INDY induced human beta cells to enter the cell cycle, both *in vitro* and *in vivo*, with beta cell labeling indices that are in the range occurring physiologically in humans during the first year of life, a range that may be relevant to therapeutic beta cell expansion[1–4]. Harmine not only induced markers of proliferation in rat, mouse and human beta cells *in vitro* but also increased beta cell mass and regeneration in a mouse PPX model and enhanced glycemic control and beta cell proliferation *in vivo* in two additional standard human islet transplant models, one euglycemic and one diabetic. Further, and unexpectedly, harmine induced production of the important beta cell transcription factors NKX6.1, PDX1 and MAFA. It appears that harmine analogs may act through the calcium-mediated, calcineurin-driven pathway, activating key cell cycle molecules such as c-MYC, CDK1, cyclins A and E, FOXM1, E2Fs and CDC25A, as well as repressing important cell cycle inhibitors such as p15^{INK4}, p16^{INK4} and p57^{CIP}. In parallel, calcineurin-NFAT signaling has also been shown to be essential in mouse genetic models of beta cell growth and differentiation[27–29].

We were surprised that DYRK1A inhibition can lead to beta cell expansion. Another group has reported that *Dyrk1a* haploinsufficiency in mice results in attenuated beta cell mass and glucose intolerance[33,34]; conversely, transgenic *Dyrk1a* overexpression leads to accentuated beta cell size, mass and proliferation, as well as enhanced glucose tolerance[35]. Potential explanations for this paradox may include differences in species, age, timing of expression (developmental phenotypes in mice versus adult treatment), duration of exposure (days in treated human islets versus permanently and constitutively in mouse genetic models), central nervous system targeting (the murine constructs affect all tissues), possible dominant-positive effects of heterozygous loss, and/or differences between drug-induced conformational changes in a given protein versus complete ablation or overexpression of the protein. Furthermore, *Dyrk1a* is an unusually complex gene, with at least nine different splice variants and up to 17 exons (nomenclature for *Dyrk1a* exons varies), only one exon of which was eliminated in the gene disruption studies[33,34]. Unraveling the gene products, cell type-specific isoforms and effects of harmine analogs on these various isoforms will require further study.

Our results support a role for DYRK1A as the relevant target of the harmine analogs and probably exclude closely related kinases such

as DYRK1B, DYRK2, DYRK3, DYRK4, and CLKs 1–4. For example, DYRKs 3 and 4 and CLKs 2 and 3 are unlikely targets because harmine analogs are weak inhibitors of these kinases, leaving DYRK1A, DYRK1B, DYRK2, CLK1 and CLK4 as the remaining likely candidates. These cannot easily be distinguished on pharmacologic grounds because the available inhibitors largely overlap. However, the complementary observations that overexpression of *DYRK1A* blocks, and silencing of *DYRK1A* mimics, the mitogenic effects of harmine and INDY on human beta cells make DYRK1A the prime candidate for a harmine analog target. Nonetheless, further specificity studies are warranted.

As DYRK and CLK family members are widely distributed, existing harmine analogs will probably have off-target effects[20–24]. For example, harmine is a CNS stimulant[36], and as noted above, it activates proliferation in alpha and ductal cells in the islet (**Supplementary Fig. 3**). Also, harmine is a peroxisome proliferator and activator of transcription-γ activator and mediator of adipogenesis in mice and leads to enhanced glucose sensitivity and disposal in obese, diabetic *db*/*db* mice, although beta cell proliferation, mass and function were not examined in that study[37]. Thus, as is the case for all potential beta cell therapeutics[25,37–40], there is an urgent need to develop strategies to deliver harmine analogs specifically to the beta cell.

In addition, understanding and optimizing the duration and dosing of future potential harmine analogs will be important, as excessive (~50- to 150-fold) *Myc* expression in mice has adverse consequences, leading to beta cell transformation, death and diabetes[11–17]. Cell death serves as an evolutionary fail-safe mechanism in all tissues that prevents accidental unrestrained production of c-MYC and tumor growth[9–14]. The observations that harmine causes only modest, twofold, increases in c-MYC, that the percentage of all beta cells (~1–1.5%) engaged in the cell cycle following harmine treatment is similar to that observed in neonatal life[1–4], and that the duration of physiologic proliferation in humans is confined to the first year or few years of life[1–4] suggest that oncogenic side effects may not occur with harmine analog treatment. The absence of evidence of beta cell death, DNA damage or dedifferentiation in response to harmine analogs is also encouraging.

In summary, harmine analogs are able to induce adult human beta cell cycle entry at rates that are in the physiologic and potentially therapeutic range. Further approaches to optimizing the potency of the harmine analog backbone, of unequivocally defining its molecular targets, and of developing methods to direct it specifically to beta cells are key future challenges.

METHODS

Methods and any associated references are available in the online version of the paper.

Note: Any Supplementary Information and Source Data files are available in the online version of the paper.

ACKNOWLEDGMENTS

The authors wish to thank R. Vasavada, N. Fiaschi-Taesch, H. Chen, K. Takane, M. Ohlmeyer, R. DeVita, E. Schadt, C. Argmann, B. Losic, D. Lebeche, S. Kim and B. Wagner for their many helpful discussions during this study. We thank the NIDDK-supported Integrated Islet Distribution Program (IIDP), T. Kin at the University of Alberta in Edmonton and P. Witkowski at the University of Chicago for providing human islets. Ad.GFP and Ad.*NFATC1* were provided by D. Lebeche (Icahn School of Medicine at Mount Sinai). This work was supported by grants from the National Institutes of Health (R-01 DK55023 (A.F.S.), U-01 DK089538 (A.F.S.), R-01 DK065149 (D.K.S.), R-01 DK067351 (A.G.-O.) and R-01 DK077096 (A.G.-O.)), the JDRF (17-2011-598 and 1-2011-603 (A.F.S.)) and the American Diabetes Association (1-14-BS-059) (A.G.-O.).

AUTHOR CONTRIBUTIONS

P.W., J.-C.A.-P., D.P.F., H.L., S.S., A.B., A.K., R.S., D.K.S., A.G.-O. and A.F.S. designed and performed experiments. P.W., A.G.-O. and A.F.S. wrote the paper.

COMPETING FINANCIAL INTERESTS

The authors declare no competing financial interests.

1. Kassem, S.A., Ariel, I., Thornton, P.S., Scheimberg, I. & Glaser, B. Beta cell proliferation and apoptosis in the developing normal human pancreas and in hyperinsulinism of infancy. *Diabetes* **49**, 1325–1333 (2000).
2. Meier, J.J. *et al.* Beta cell replication is the primary mechanism subserving the postnatal expansion of beta cell mass in humans. *Diabetes* **57**, 1584–1594 (2008).
3. Köhler, C.U. *et al.* Cell cycle control of beta cell replication in the prenatal and postnatal human pancreas. *Am. J. Physiol. Endocrinol. Metab.* **300**, E221–E230 (2011).
4. Gregg, B.E. *et al.* Formation of a human beta cell population within pancreatic islets is set early in life. *J. Clin. Endocrinol. Metab.* **97**, 3197–3206 (2012).
5. Butler, A.E. *et al.* Beta cell deficit and increased beta cell apoptosis in humans with diabetes. *Diabetes* **52**, 102–110 (2003).
6. Saisho, Y. *et al.* Beta cell mass and turnover in humans: effects of obesity and aging. *Diabetes Care* **36**, 111–117 (2013).
7. Kulkarni, R.N., Bernal-Mizrachi, E., Garcia-Ocaña, A. & Stewart, A.F. Human β-cell proliferation and intracellular signaling: driving in the dark without a roadmap. *Diabetes* **61**, 2205–2213 (2012).
8. Bernal-Mizrachi, E., Kulkarni, R.N., Stewart, A.F. & Garcia-Ocaña, A. Human β-Cell proliferation and intracellular signaling part 2: still driving in the dark without a roadmap. *Diabetes* **63**, 819–831 (2014).
9. Soucek, L. & Evan, G.I. The ups and downs of Myc biology. *Curr. Opin. Genet. Dev.* **20**, 91–95 (2010).
10. Wierstra, I. & Alves, J. The *c-myc* promoter: still *M*yster*Y* and *C*hallenge. *Adv. Cancer Res.* **99**, 113–333 (2008).
11. Bretones, G., Delgado, M.D. & Leon, J. Myc and cell cycle control. *Biochim. Biophys. Acta* doi:10.1016/j.bbagrm.2014.03.013 (2014).
12. Pelengaris, S., Kahn, M. & Evan, G.I. Suppression of myc-induced apoptosis in beta cells exposes multiple oncogenic properties of myc and triggers carcinogenic progression. *Cell* **109**, 321–334 (2002).
13. Pelengaris, S. & Khan, M. Oncogenic co-operation in β-cell tumorigenesis. *Endocr. Relat. Cancer* **8**, 307–314 (2001).
14. Finch, A. *et al.* Bcl-X_L gain of function and $p19^{ARF}$ loss of function cooperate oncogenically with Myc *in vivo* by distinct mechanisms. *Cancer Cell* **10**, 113–120 (2006).
15. Laybutt, D.R. *et al.* Overexpression of c-myc in beta cells of transgenic mice causes proliferation and apoptosis, downregulation of insulin gene expression and diabetes. *Diabetes* **51**, 1793–1804 (2002).
16. Cano, D.A. *et al.* Regulated beta-cell regeneration in the adult mouse pancreas. *Diabetes* **57**, 958–966 (2008).
17. Karslioglu, E. *et al.* cMyc is the principal upstream driver of beta cell proliferation in rat insulinoma cell lines and Is an effective mediator of human beta cell replication. *Mol. Endocrinol.* **25**, 1760–1772 (2011).
18. Chung, N. *et al.* Median absolute deviation to improve hit selection for genome-scale RNAi screens. *J. Biomol. Screen.* **13**, 149–158 (2008).
19. Goktug, A.N., Chai, S.C.C. & Chen, T. Data analysis approaches in high throughput screening. in *Drug Discovery* Ch. 7, doi:10.5772/52508 (2013).
20. Becker, W. & Sippl, W. Activation, regulation and inhibition of Dyrk1a. *FEBS J.* **278**, 246–256 (2011).
21. Ogawa, Y. *et al.* Development of a novel selective inhibitor of the Down syndrome-related kinase Dyrk1a. *Nat. Commun.* **1**, 86 10.1038/ncomms1090 (2010).
22. Tahtouh, T. *et al.* Selectivity, co-crystal structures and neuroprotective properties of leucettines, a family of protein kinase inhibitors derived from the marine sponge alkaloid leucettamine B. *J. Med. Chem.* **55**, 9312–9330 (2012).
23. Walte, A. *et al.* Mechanism of dual specificity kinase activity of Dyrk1a. *FEBS J.* **280**, 4495–4511 (2013).
24. Jain, P. *et al.* Human cdc2-like kinase 1 (CLK1): a novel target for Alzheimer's disease. *Curr. Drug Targets* **15**, 539–550 (2014).
25. Shen, W. *et al.* Small molecule inducer of beta cell proliferation identified by high-throughput screening. *J. Am. Chem. Soc.* **135**, 1669–1672 (2013).
26. Gallo, E.M., Cante-Barrett, K. & Crabtree, G.R. Lymphocyte calcium signaling from membrane to nucleus. *Nat. Immunol.* **7**, 25–32 (2006).
27. Heit, J.J. *et al.* Calcineurin/NFAT signaling regulates pancreatic β-cell growth and function. *Nature* **443**, 345–349 (2006).
28. Goodyer, W.R. *et al.* Neonatal beta cell development in mice and humans is regulated by calcineurin/NFaT. *Dev. Cell* **23**, 21–34 (2012).
29. Demozay, D., Tsunekawa, S., Briaud, I., Shah, R. & Rhodes, C.J. Specific glucose-induced control of insulin receptor-supstrate-2 expression is mediated by Ca^{2+}-dependent calcineurin-NFAT signaling in primary pancreatic islet β-cells. *Diabetes* **60**, 2892–2902 (2011).
30. Nica, A.C. *et al.* Cell-type, allelic and genetic signatures in the human pancreatic beta cell transcriptome. *Genome Res.* **23**, 1554–1562 (2013).

31. Wang, H. *et al.* Improved low molecular weight Myc-Max inhibitors. *Mol. Cancer Ther.* **6**, 2399–2408 (2007).
32. de Alboran, I.M. *et al.* Analysis of cMYC function in normal cells via conditional gene-targeted mutation. *Immunity* **14**, 45–55 (2001).
33. Fotaki, V. *et al.* Dyrk1a haploinsufficiency affects viability and causes developmental delay and abnormal brain morphology in mice. *Mol. Cell. Biol.* **22**, 6636–6647 (2002).
34. Rachdi, L. *et al.* Dyrk1a haploinsufficiency induces diabetes in mice through decreased pancreatic beta cell mass. *Diabetologia* **57**, 960–969 (2014).
35. Rachdi, L. *et al.* Dyrk1a induces pancreatic beta cell mass expansion and improves glucose tolerance. *Cell Cycle* **13**, 2221–2229 (2014).
36. Brierley, D.I. & Davidson, C. Developments in harmine pharmacology – implications for ayahuasca use and drug-dependence treatment. *Prog. Neuropsychopharmacol. Biol. Psychiatry* **39**, 263–272 (2012).
37. Waki, H. *et al.* The small molecule harmine is an antidiabetic cell-type specific regulator of PPARγ expression. *Cell Metab.* **5**, 357–370 (2007).
38. Purwana, I. *et al.* GABA promotes human beta-cell proliferation and modulates glucose homeostasis. *Diabetes* **63**, 4197–4205 (2014).
39. Wang, W. *et al.* Identification of small molecule inducers of pancreatic beta cell proliferation. *Proc. Natl. Acad. Sci. USA* **106**, 1427–1432 (2009).
40. Chamberlain, C.E. *et al.* Menin determines K-Ras proliferative outputs in endocrine cells. *J. Clin. Invest.* **124**, 4093–4101 (2014).

ONLINE METHODS

General experimental approaches. No samples, mice or data points were excluded from the reported analyses. For islet studies, equivalent aliquots of every islet batch were randomly assigned to culture wells or microscope slides. For mouse studies, mice were randomly selected to groups to receive harmine or vehicle control or to receive partial pancreatectomy or sham pancreatectomy. Some analyses were not performed in a blinded fashion. See "Statistical analyses" below for more detail.

Reagents. Reagents were as follows: INDY (4997, Tocris Biosciences), BrdU (RPN20, GE Healthcare), harmaline (51330, Sigma), harmane (103276, Sigma), harmalol (H125, Sigma), harmine (286044, Sigma, for *in vitro* studies), harmine hydrochloride (CAS 343-27-1, Santa Cruz, for *in vivo* studies), VIVIT (502306392, Fisher scientific), FK506 (tlrl-fk5, Invivogen), 1RH (10058, 475956, Calbiochem), etoposide (E1383, Sigma), recombinant human IL-1β (201-lb-005, R&D Systems), recombinant human TNF-α (210-TA-010, R&D Systems), WS6 (M60097-2s, Xcess Biosciences).

Cell lines. Four cell lines were initially assessed for the HTS: rat insulinoma cells (Ins1 823/13), mouse insulinoma cells (βTC3), human hepatoma cells (HepG2) and human colon cancer cells (HCT116). The human hepatoma cell line used for these studies, HepG2 (ATCC), was cultured in EMEM medium supplemented with 10% FCS, 1% penicillin-streptomycin. The adenovirus packaging cell line, HEK-293A (Life Technologies), was cultured in DMEM medium supplemented with 10% FCS, and 1% penicillin-streptomycin, and 1× MEM containing non-essential amino acids. Cell lines were not validated by genomic testing and were not tested for mycoplasma.

Generation of stable cell lines. HepG2 cells, βTC3 cells, Ins1 823/13 cells and HCT116 cells were transduced in T25 flasks with plasmid DNA encoding the *MYC* promoter–driven luciferase reporter construct described below. After transfection for 48 h, the cells were trypsinized and re-seeded using serial dilution into 96-well plates containing 1 μg ml^{-1} puromycin for selection. After 3 weeks, individual clones were picked and reconsolidated into 24-well plates. Clones were verified as containing the plasmid by luciferase activity.

Small-molecule screening. A 2.5-kb human *MYC* promoter plasmid was obtained from Addgene[41]. The *MYC* promoter fragment was excised with SacI and HindIII and ligated into the PGL4.20 luciferase vector (Promega). This was stably introduced into HepG, βTC3, Ins1 823/13 and HCT116 cell lines. HepG2 cell clone 13 (**Supplementary Fig. 1**) was ultimately selected for the screen because of its stability and robust response (Z′ of 0.75)[18,19,42] to the positive controls, IL1-β and TNF-α, in a preliminary screen. These cells were maintained in complete DMEM medium with 1μg ml^{-1} puromycin. As a positive control, a combination of IL-1β and TNF-α was selected because of the NF-κB sites in the *MYC* promoter.

Screening was carried out in 384-well format using two commercially sourced libraries. The FDA library (2,300 compounds, Microsource Discovery Systems), composed of compounds approved for use in humans or animals, was used in a pilot screen, and to evaluate the robustness of the assay format. The L1 library (100,000 compounds; Chembridge) is composed of a structurally diverse set of small molecules selected based on their adherence to Lipinski's rule of 5 (ref. 43), an indication of drug-like properties based on small-molecule structure. All library compounds are stored as 10-mM stocks (DMSO).

For screening, 384-well assay plates (PerkinElmer ProxiPlate 6008230) were pre-filled with HepG2 cells (5,000 cells/well in 10 μl) expressing the luciferase reporter construct. Twenty-four hours after cell addition, compounds from library plates were transferred by pin tool (V&P Scientific) into assay plates at a final concentration of 7.5 μM. As positive control, 1 μl IL-1β was added at a final assay concentration of 5 ng ml^{-1} (Multidrop Combi; Thermo Scientific). Following 24 h of incubation, luciferase expression was evaluated by the addition of 5 μl luciferase substrate reagent (Neolite PerkinElmer); luminescence was detected after 10 min using an EnVision plate reader (PerkinElmer).

Assay plates were validated using Z-factor (0.5 cutoff)[42] comparing positive-control wells to blank wells. Data were normalized against plate controls using normalized percentage activation (NPA)[19]. A subset of 86 positive compounds showing an NPA >15% was selected for secondary screens and IC_{50} determination in primary beta cells based on proliferation. Additionally, the entire data set was renormalized using Robust Z-score (a method developed for the analysis of RNAi screens)[18], and compounds showing a score >3 median absolute deviation (MAD) above the background signal were used for ranked scoring in subsequent structure-activity relationship (SAR) analysis. (Compounds with a Robust Z-score <3 MAD were considered to be negative).

Human, rat and mouse islets. Human islets from 63 donors were obtained through the NIH-supported Integrated Islet Distribution Program (IIDP). The islets were harvested from deceased donors without any identifying information at NIH-approved centers with informed consent and IRB approval at the islet-isolating centers. Donors ranged in age from 18 to 69 years (mean 43.5); 28 were female, 35 were male. There was no relationship between age and the ability of harmine to activate proliferation within these age constraints. Mean BMI was 29.4 (range 15–44), and cold ischemia time was 635 min (range 121–1,150). Purity ranged from 50% to 95%. Rat islets were isolated from 8- to 10-week-old male Wistar rats (Charles River Laboratories, Wilmington, MA) as described previously[44,45]. Mouse islets were isolated from 8- to 10-week-old male and female $Myc^{loxP/loxP}$ mice[32]. Isolated rat and mouse islets were cultured in RPMI 1640 medium (Life Technologies) containing 10% FCS, 5.5 mM glucose, and 1% penicillin-streptomycin for 24 h. Islets were dispersed by trypsinization. All animal studies were performed in compliance with, and with approval of, the Icahn School of Medicine at Mount Sinai Institutional Animal Care and Use Committee.

Islet dispersion. Islets were dispersed as described[46–49], centrifuged at 1,500 r.p.m. for 10 min, washed twice in PBS, resuspended in 1 ml of 1 mg ml^{-1} trypsin, and incubated for 10 min at 37 °C. During this digestion, the islets were dispersed by gentle pipetting up and down every 5 min for 10 s. Complete RPMI medium containing 5.5 mM glucose, 1% penicillin/streptomycin with 10% FBS was then added to stop the digestion. The cells were then centrifuged for 5 min at 1,500 r.p.m., the supernatants removed, the pellet resuspended in complete medium, and cells then plated on coverslips with 50 μl cell suspension per coverslip. For rat islets, poly-D-lysine/laminin-treated cover slides were used. Cells were then allowed to attach for 2 h at 37 °C or were transduced with adenovirus for 2 h. For $Myc^{loxP/loxP}$ mouse islet studies, islets were isolated and dispersed on poly-D-lysine/laminin-treated cover slips and transduced with Ad.Lacz or Ad.Cre. After 2 h, 500 μl complete RPMI medium was added in each well to terminate the adenoviral transduction. Cells were cultured for 48–96 h as described in the figure legends.

Compound treatments. For compound treatment, after dispersed islets were allowed to recover from dispersal on coverslip 24 h, complete medium was replaced with the medium containing compounds for 3–96 h. Specifically, for Ki-67 staining and BrdU staining, the cells were treated with compounds for 72 h, and BrdU labeling was for 72 h. For phospho–histone-3 staining, the cells were treated with compounds for 96 h. For Ad.*NFATC1*-GFP nuclear translocation, the cells were transduced with adenovirus for 48 h, after which cells were treated with harmine or INDY for 3 h. For inhibitor experiments with VIVIT or FK506, cells were pretreated with inhibitor for 2 h before addition of harmine or INDY.

Immunocytochemistry. Islet cells on coverslips were fixed in fresh 4% paraformaldehyde for 15 min at 25 °C, washed with PBS and incubated in blocking buffer (1.0% BSA, 0.5% Triton, and 5% normal goat serum (NGS) in PBS) for 1 h at 25 °C. Cells on coverslips were incubated with primary antisera overnight at 4 °C in blocking buffer. Secondary antisera were added for 1 h at 25 °C in secondary buffer (1% BSA, 0.5% Triton in PBS, 5% NGS). For phosphohistone-3 and phospho-γ-H2AX, primary antibody was exposed 2 h at 25 °C. TUNEL labeling was performed according to Promega instructions (G3250, Promega). BrdU immunocytochemistry was performed using 1N HCL antigen-retrieval for 30 min at 37 °C after fixation. Primary antisera were as follows: BrdU (ab6326, Abcam, 1:300), Ki-67 (RM-9106-s1, Thermo Scientific, 1:300), p-Histone-3 (06-570, Millipore, 1:500), insulin (A0564, DAKO, 1:500), NFAT1 (ab2722, Abcam, 1:100), NFAT2 (556602, BD Pharmingen, 1:100), NFAT3

(Sc-13036, Santa Cruz, 1:100), NFAT4 (Sc-8321, Santa Cruz, 1:100), p-γH2AX (MA1-2022 Thermo Scientific, 1:500), DYRK1A (D-1694, Sigma, 1:100), FoxM1 (Sc-500 Santa Cruz, 1:100), p57 (2557s, Cell Signaling, 1:100), E2F2 (Sc-632, Santa Cruz, 1:100), Nkx6.1 (F55A10-c, University of Iowa, 1:300), Pdx1 (07-696, Millipore, 1:300), MafA (Ab26405, Abcam, 1:200), glucagon (2760s Cell Signaling, 1:300), somatostatin (Sc-20999, Santa Cruz, 1:300), pancreatic polypeptide (A0619, DAKO, 1:300), CK19 (Ab52625, Abcam, 1:300). Labeled cells were then visualized using laser confocal microscopy (Leica SP5 DM). TUNEL labeling was performed using the DeadEnd Fluormetric TUNEL System (Cat#G3250, Promega). Results shown are representative of three to six separate human or rat islet preparations. For islets from each donor or animal, we took 10–20 photomicrographs of the islets on the coverslips and counted the beta cells in the images. The number of photos taken depended on the density of cells on the coverslips, but enough was read to examine a minimum of 1,000 beta cells in total per group.

Immunoblotting. Islet extracts (20–50 μg) were resolved using 10% or 12% SDS-PAGE and transferred to Immobilon-P membranes (Millipore). Primary antisera included c-MYC (9402, Cell Signaling, 1:1,000), α-tubulin (CP06, Calbiochem, 1:2,000), DYRK1A (D-1694, Sigma, 1:1,000), Cdk1 (Sc-747, Santa Cruz, 1:1,000), cyclin A (Sc-239,Santa Cruz, 1:500), cyclin E (Sc-481, Santa Cruz, 1:500), FoxM1(Sc-500 Santa Cruz, 1:500), $p16^{INK4a}$ (Sc-468, Santa Cruz, 1:1,000), $p57^{CIP2}$ (2557s, Cell Signaling, 1:1,000), E2F1 (Sc-193, Santa Cruz, 1:1,000), E2F2 (Sc-632, Santa Cruz, 1:1,000), Nkx6.1 (F55A10-c, University of Iowa, 1:1,000), Pdx-1 (07-696, Millipore, 1:1,000), MafA (Ab26405, Abcam, 1:1,000), GAPDH (Sc-25778, Santa Cruz, 1:1,000). Quantitative densitometry was performed using Image J software (NIH).

Gene expression. RNA was isolated and quantitative RT-PCR was performed as described previously[46]. Gene expression in dispersed islets or cell lines was analyzed by real-time PCR performed on an ABI 7500 System. Primer sequences are in **Supplementary Table 1**.

Plasmids and adenoviruses. Ad.GFP and Ad.*NFATC1* were provided by D. Lebeche (Icahn School of Medicine at Mount Sinai). Ad.*DYRK1A* was made using the pAd/CMV/V5-DEST Gateway recombination system (Life Technologies) after cloning the human full-length *DYRK1A* into the pENTR vector. An Ad.shRNA directed against human *DYRK1A* was prepared using the Block-It RNAi kit (Life Technologies) targeting *GGAACTTAAAGAAGACCAAAG* using the U6 promoter). Adenoviruses were packaged and produced in HEK-293A cells. Titers were determined by plaque assay (PFU). Dispersed rat or human islets on coverslips were transduced with either experimental or control adenoviruses (Ad.Cre, Ad.Scrambled, or Ad.LacZ) at 200 MOI in serum-free medium for 2 h. Transduction was stopped by adding complete medium containing 10% FCS and cultured for 48 to 96 h as described in the figures.

Glucose-stimulated insulin secretion and insulin content. Insulin release was measured in triplicate from human islets treated either with vehicle (DMSO), harmine or INDY for 72 h[46–49]. Briefly, islets were preincubated in Krebs-Ringer bicarbonate buffer supplemented with 10 mmol/l HEPES, 1% BSA, and 2.8 mmol/l glucose for 1 h at 37 °C in a 5% CO_2 incubator, then treated with harmine or INDY for 24 h. After washing once with the same solution, groups of 15 islet equivalents (IEQs) per condition were incubated in 1 ml fresh Krebs-Ringer bicarbonate buffer plus 1% BSA and either 2.8 or 16.7 mmol/l glucose for 30 min. Buffer was removed and frozen at −20 °C for insulin measurement by insulin ELISA kit (EZHI-14K, Millipore). Islets were then digested overnight in NaOH at 37 °C, and protein was measured by the Bradford method after neutralization with HCl. Insulin values are normalized to protein content.

Mouse partial pancreatectomy model (PPX). This model has been described in detail[50,51]. Briefly, 2- to 3-month-old male C57BL/6 mice were randomized into two groups (PPX or sham PPX), and a 60% PPX (splenic portion) ($n = 16$) or sham PPX (laparotomy only) ($n = 16$) was performed. Following PPX, mice were allowed to recover for 24 h, and then further randomized to receive vehicle (saline) or 10 mg kg^{-1} harmine HCl by intraperitoneal injection daily for 7 or 14 d. They were killed on day 7 ($n = 8$) for Ki-67 studies or on day 14 ($n = 8$) for beta cell mass determination. Beta cell mass and islet number were measured in four insulin-stained pancreas sections per mouse using ImageJ software (National Institutes of Health, Bethesda, MD)[51]. Sections were also stained for Ki-67 and insulin. A minimum of 2,000 beta cells per pancreas were counted. Investigators were blinded as to group assignments.

Euglycemic human islet transplantation model. 1,000 human islet equivalents (IEQ) from three different human cadaveric donors were transplanted under the renal capsule of six euglycemic 3-month-old NOD-SCID mice as detailed previously[47–49]. Animals were allowed to recover for 7 d and were then randomly selected to be given 10 mg kg^{-1} harmine HCl intraperitoneally ($n = 3$) or vehicle (saline) ($n = 3$) every 12 h for 7 d as described by Waki[37]. On the evening of day 13, animals were given BrdU intraperitoneally, and in the morning of day 14, animals were killed and kidneys harvested, fixed, embedded, sectioned and immunostained for insulin and BrdU as detailed previously[47–49]. BrdU incorporation in the controls was 0.12% ± 0.08%; beta cell Ki-67 labeling in the controls was 0.22% ± 0.07%. Investigators were blinded as to group assignments.

Diabetic marginal mass human islet transplantation model. 500 IEQ from four different donors were transplanted under the renal capsule of 7 male NOD-SCID mice rendered diabetic by 200 mg kg^{-1} streptozotocin as detailed previously[47–49]. Mice were randomly selected for treatment with 10 mg kg^{-1} harmine HCl ($n = 4$) or saline ($n = 3$) as above. Blood glucose was at least 400 mg dl^{-1} before islet transplant and was measured daily following transplant. An intraperitoneal glucose tolerance test (2 mg kg^{-1})[47–49] was performed on day 21, and islet grafts were excised by unilateral nephrectomy (UNX) as described in detail[47–49]. Investigators were blinded as to group assignments.

Statistical analyses. All mouse and *in vitro* experiments were repeated multiple times in multiple batches of mouse, rat and human islets as indicated in the figure legends, and were analyzed in a blinded manner at the conclusion of the experiment. Key analyses from one author were repeated in a blinded manner by another author. All data are expressed as the mean ± s.e.m. Results were accepted as statistically significant at $P < 0.05$, as determined using two-tailed Wilcoxon rank test or Student's unpaired *t*-test as indicated in the figures and legends. Sample size was based on prior studies in which 3–7 sets of human or rat islets were used[45–49,51]. A minimum of 1,000 beta cells were counted for each graph shown.

41. He, T.C. *et al.* Identification of cMyc as a target of the APC pathway. *Science* **281**, 1509–1512 (1998).
42. Zhang, J.H., Chung, T. & Oldenburg, K. A simple statistical parameter for use in evaluation and validation of high throughput screening assays. *J. Biomol. Screen.* **4**, 67–73 (1999).
43. Lipinski, C.A., Lombardo, F., Dominy, B.W. & Feeney, P.J. Experimental and computational approaches to estimate solubility and permeability in drug discovery and development settings. *Adv. Drug Deliv. Rev.* **46**, 3–26 (2001).
44. Ricordi, C. & Rastellini, C. Methods in pancreatic islet separation. in *Methods in Cell Transplantation* (ed. Ricordi, C.) 433–438 (R.G. Landes Co, Austin, Texas), (2000).
45. Cozar-Castellano, I. *et al.* Lessons from the first comprehensive molecular characterization of cell cycle control in rodent insulinoma cell lines. *Diabetes* **57**, 3056–3068 (2008).
46. Metukuri, M.R. *et al.* ChREBP mediates glucose-stimulated pancreatic beta cell proliferation. *Diabetes* **61**, 2004–2015 (2012).
47. Fiaschi-Taesch, N.M. *et al.* Hepatocyte growth factor (HGF) enhances engraftment and function of non-human primate islets. *Diabetes* **57**, 2745–2754 (2008).
48. Fiaschi-Taesch, N.M. *et al.* A survey of the human pancreatic beta cell G1/S proteome reveals a potential therapeutic role for cdk-6 and cyclin D_1 in enhancing human beta cell replication and function *in vivo*. *Diabetes* **58**, 882–893 (2009).
49. Fiaschi-Taesch, N. *et al.* Induction of human beta cell proliferation and engraftment using a single G1/S regulatory molecule, cdk6. *Diabetes* **59**, 1926–1936 (2010).
50. Peshavaria, M. *et al.* Regulation of pancreatic beta cell regeneration in the normoglycemic 60% pancreatectomy mouse. *Diabetes* **55**, 3289–3298 (2006).
51. Alvarez-Perez, J.C. *et al.* Hepatocyte growth factor/c-Met signaling is required for β-cell regeneration. *Diabetes* **63**, 216–223 (2014).

doi:10.1038/nm.3820